


Article

# euAP2a, a key gene that regulates flowering time in peach (*Prunus persica*) by modulating thermo-responsive transcription programming

Jiayang Liu, Dennis Bennett, Mark Demuth, Erik Burchard, Tim Artlip , Chris Dardick\* and Zongrang Liu\*

USDA-ARS, Appalachian Fruit Research Station, 2217 Wiltshire Road, Kearneysville, WV 25430, USA

\*Corresponding authors. E-mails: [chris.dardick@usda.gov](mailto:chris.dardick@usda.gov); [zongrang.liu@usda.gov](mailto:zongrang.liu@usda.gov)

## Abstract

Frequent spring frost damage threatens temperate fruit production, and breeding of late-flowering cultivars is an effective strategy for preventing such damage. However, this effort is often hampered by the lack of specific genes and markers and a lack of understanding of the mechanisms. We examined a Late-Flowering Peach (*LFP*) germplasm and found that its floral buds require a longer chilling period to release from their dormancy and a longer warming period to bloom than the control cultivar, two key characteristics associated with flowering time. We discovered that a 983-bp deletion in *euAP2a*, an *APETALA2* (*AP2*)-related gene with known roles in regulating floral organ identity and flowering time, was primarily responsible for late flowering in *LFP*. This deletion disrupts an miR172 binding site, resulting in a gain-of-function mutation in *euAP2a*. Transcriptomic analyses revealed that at different stages of floral development, two chilling-responsive modules and four warm-responsive modules, comprising approximately 600 genes, were sequentially activated, forming a unique transcription programming. Furthermore, we found that *euAP2a* was transiently downregulated during the activation of these thermal-responsive modules at various stages. However, the loss of such transient, stage-specific downregulation of *euAP2a* caused by the deletion of miR172 binding sites resulted in the deactivation or delay of these modules in the *LFP* flower buds, suggesting that *euAP2a* acts as a transcription repressor to control floral developmental pace in peaches by modulating the thermo-responsive transcription programming. The findings shed light on the mechanisms behind late flowering in deciduous fruit trees, which is instrumental for breeding frost-tolerant cultivars.

## Introduction

Spring frost can cause significant damage to temperate tree fruits like peach and apple, leading to occasional catastrophic losses to growers. This threat has been exacerbated by ongoing global climate change, leading to warmer winter temperatures and increased temperature fluctuations during late winter and early spring. Currently, spring frosts or freezes can only be mitigated to a limited extent with mechanical measures, such as wind machines, helicopters, heaters, sprinklers etc [1]. One of the promising horticultural solutions is to breed late-flowering cultivars to avoid spring frost. However, this trait is often scarce in the germplasm pool, or is linked with undesired traits, making the breeding process lengthy and laborious. It is therefore important to search for and characterize novel late-flowering traits and the underlying regulatory mechanism.

The floral cycle in annuals begins with the transition from vegetative to inflorescence stage and typically completes within a single growing season [2, 3]. In contrast, temperate fruit trees experience a more complex process, which involves flower initiation and development being interrupted by seasonal thermal regimes [4]. For example, apple and peach trees can remain in a juvenile phase for 3 to 6 years, during which flower initiation is inhibited. In adult trees, flower initiation, development, and flowering span across two growing seasons and are subjected to

temperature-dependent regulations. Typically, floral bud initiation occurs in summer and rudimentary morphological structures such as sepal, petal, stamen, and carpel are developed throughout fall before entering a fully dormant state. This dormant bud is irresponsive to growing conditions unless exposed to a certain period of chilling temperatures (0–7.5°C; [5]). The chilling requirement (CR) for this process varies greatly across cultivars and genotypes [6]. QTL mapping indicates that CR is genetically controlled, and CR related genes are tightly linked with genes controlling bloom date [7]. Interestingly, CRs can also differ among buds on the same tree and different floral organs from the same flower, indicating that CR is also influenced by physiological states and spatiotemporal developmental fate of meristematic cells [8–10].

In fact, chilling acts as a key biological regulator to drive floral buds through critical developmental stages. Floral buds in apple and peach, despite the lack of visible change in form and size over winter chilling, undergo internal changes and tissue differentiation, such as the development of epidermis, endothecium, middle layers, microsporangium walls, tapetum, pollen mother cells, ovules, and vascular connections between floral primordia and branch wood [11–16]. Insufficient chilling, however, leads to the partial arrest of these tissues' development [10, 17], while warm/ambient growth conditions hardly induce such

Received: 28 September 2023; Accepted: 5 March 2024; Published: 8 April 2024 Corrected and Typeset: 1 May 2024

Published by Oxford University Press on behalf of Nanjing Agricultural University. This work is written by (a) US Government employee(s) and is in the public domain in the US.

morphological changes [18]. These findings highlight chilling-induced internal sporogenous tissues as a morphological indicator marking a complete transition from endodormancy to ecodormancy. As such, insufficient chilling in warm winter often slows down or impedes floral development and bloom time [19], while overchilling often leads to a shortening of the flowering time due to an overdrive of floral development by chilling for an extended period [20–22]. Thus, the effects of chilling on reshaping the dormant state places the dormancy progression within the context of floral development.

Once the chilling requirement is fulfilled, the floral bud becomes competent in response to warming temperatures in spring, resuming its developmental course as characterized by enlargement of floral organs and successive proceeding of sporogenesis and gametogenesis followed by anthesis, pollination, fertilization, and fruit setting events [11, 15, 16, 23]. Floral development or flowering time is temperature-dependent, with fast development accelerated at higher temperatures. However, this thermal response differs greatly among genotypes. An investigation of 136 peach cultivars indicates a wide spectrum of heat requirement (HR) for blooming, ranging from 1362 to 10 348 growing degree hours (GDHs), a measure of heat amount accumulated between CR completion and bloom date [24–26]. Like CR, HR is under genetic control and a key trait directly relevant to blooming time. [27–29]. However, the genes that control flowering time and the exact regulatory mechanism in fruit trees remain largely unknown. In *Arabidopsis*, warm temperature-mediated elongation growth and flowering is dependent on *PHYTOCHROME INTERACTING FACTOR4* (*PIF4*) [30, 31]. *PIF4* factor orchestrates the transcriptional activity of numerous genes related to cell elongation, thermal-responsive growth, shade avoidance and flowering [32]. The transcriptional response of *PIF4* to ambient temperature is mediated by two distinct thermosensors: the evening complex (EC) and phytochrome B (PhyB). EC is a transcriptional repressor composed of three proteins, *EARLY FLOWERING3* (*EFL3*), *ELF4*, and *ARRHYTHMO* (*LUX*), and directly binds to the *PIF4* promoter and represses it at low temperature. *ELF3* is the only thermal responsive factor whose activity depends on temperature and becomes less active at high temperature, resulting in reduction or loss of the EC binding to the *PIF4* promoter or higher *PIF4* transcription [33–35]. PhyB binds to the *PIF4* promoter, and its regulatory action is largely dependent on its active/inactive state, which is orchestrated by light and ambient temperature. Under light condition, PhyB is active and represses *PIF4* transcription, but higher temperatures reverse the active to inactive state, leading to de-repression of *PIF4* [36]. Taken together, the thermosensors and *PIF4* are key thermal factors that regulate bloom time, which should be instrumental for understanding of flowering time regulation in fruit trees.

Recent progress in our peach breeding program for later blooming traits have led to the development of a new germplasm, the Late-Flowering Peach (*LFP*), which blooms about 10 days to two weeks later than all other peach cultivars grown in the Kearneysville, WV area (39.3578 N, –77.8845 W). This delayed bloom time has the potential to increase the success of peach cultivation in the region by avoiding spring frosts. To better understand the genetic basis of this trait, we characterized the late-flowering trait and its thermal response, and identified a deletion mutation in one of the genes that exhibited differential expression in *LFP* plants when compared to a control peach that has a typical bloom date. Through comprehensive genomic and transcriptomic analyses, we successfully pinpointed a specific deletion within the peach *euAP2a* gene that is responsible for the delayed flowering

characteristic in *LFP* peach. Further investigations have revealed the complex and thermos-responsive transcriptional programming by which *euAP2a* governs floral development pace.

## Results

### Characterization of a late-flowering peach line

The late-flowering peach (*LFP*; KV021779) was selected in an F1 population of an open-pollinated KV981056, which is an F1 progeny of a cross between KV930465 and KV910437 (Fig. 1a). This late-flowering phenotype was not observed in either of the parent lines and the original source of the trait remains unknown. The *LFP* flower also displays an increase in floral organs, with an average of 8 to 10 sepals and 25 to 30 petals compared to 5 of each in wild type peach cultivars, 60 to 70 stamens compared to 35 to 45 in wild type peach cultivars, and often two pistils (Fig. 1k–m). Under the climate in Kearneysville, the *LFP* tree flowers near the end of April, which is about two weeks later than other Wt peach cultivars, but very close to the average last day when frost damage risk occurs in the region.

### *LFP* required a longer chilling period to release from dormancy

In *Prunus* and other fruit trees, the chilling period required for breaking dormancy is known to be correlated with bud break time [21, 22, 25]. To test whether *LFP* acquires an intrinsically longer chilling period, we chilled the *LFP* floral buds together with Wt control 'John Boy' (*JB*) as described previously [37] for various periods before transferring them to warm conditions (18–22°C) to force flowering. Fig. 1 shows that the *LFP* floral buds required a longer chilling period. The *JB* floral buds showed budbreak after exposure to 800 chilling hours (CH; Fig. 1f), but the *LFP* buds did not show it until 1000 CH (Fig. 1k), indicating that the *LFP* requires at least 200 CH more than the *JB* buds. As expected, the *LFP* floral buds produced more sepals, petals, and stamens (Fig. 1k, m) compared to the *JB* floral buds (Fig. 1l), consistent with its phenotype observed under field conditions.

### The *LFP* floral buds required longer warm exposure for flowering

Previous studies have revealed a correlation between budbreak time and heat requirement [21, 22, 25]. While *LFP* showed a drastic delay of flowering in the spring, the exact warm period required for flowering was not yet determined. When kept at temperatures between 18°C and 22°C, *JB* flower buds showed no morphological changes until Day 16, when visible bud enlargement occurred, followed by budbreak on Day 20. However, the *LFP* buds had a slow morphological response, and no visible enlargement was observed until Day 24, before the eventual budbreak on Day 28 (Fig. 2), which was 8 days later than *JB*. This finding confirmed the late flowering behavior of the *LFP* buds as observed in the field.

### The *LFP* floral buds flower retained intact thermal responses but in a slow pace

The flowering of annuals is thermally dependent and occurs rapidly at high ambient temperatures and slowly at low temperatures [31]. To understand the thermal dependence of peach flowering and the response of the *LFP* floral buds to different temperatures, we evaluated the budbreak and bloom time at 10°C, 15°C and 25°C in optimal growth chamber conditions (Fig. 3a). The fully chilled *JB* floral buds flowered quickly at 25°C, blooming as early as Day 6, and more slowly at 15°C and 10°C. In contrast, the *LFP* floral buds showed a delayed response to the same warm

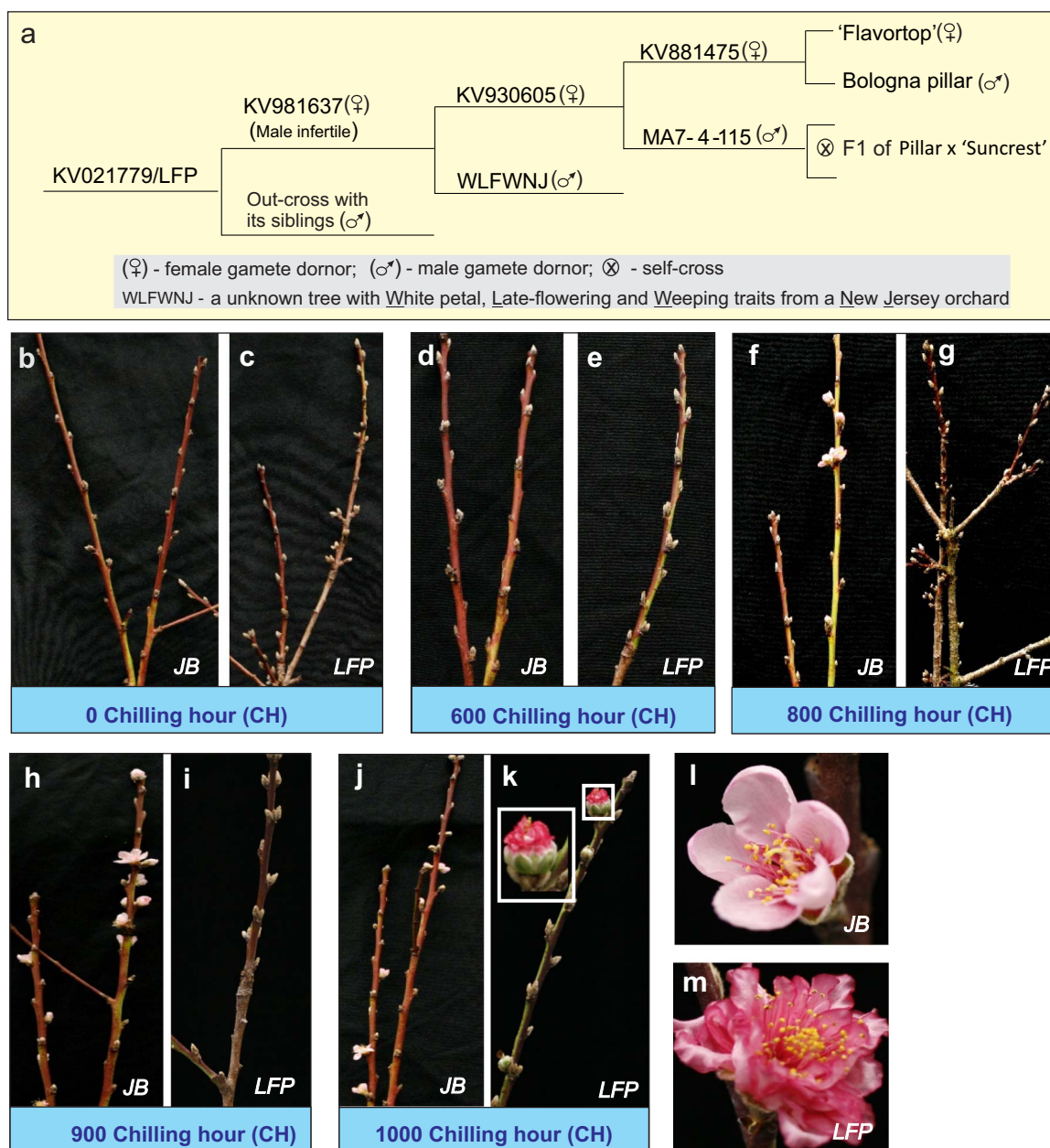


**Figure 1.** The pedigree of the late-flower peach (LFP) and its chilling requirement. **(a)** The LFP peach was derived from a series of indicated crosses. **(b-m)** Shoots with full dormant buds from “John Boy” (JB) (b, d, f, h, j, l) and LFP (c, e, g, i, k, m) trees were collected and subjected to chilling treatment at 4°C for up to 1000 hours (CH) to fulfill chilling requirement, followed by warm growth condition (~18-22°C) to induce bloom. An enlarged image of a LFP flower is presented in a separate inset (k).

temperatures, with a 10-day delay in blooming at 25°C and a 15-day delay in bud break at 15°C, and a much longer delay at 10°C compared to the JB floral buds (Fig. 3a). This indicates that the LFP floral buds are capable of responding differently to various warm temperature stimuli but at a slower pace, which is in contrast to *Arabidopsis* mutants in which the temperature-dependent flowering response is lost due to mutation [31–35]. It is also noted that the LFP flowered much later at low temperatures (10°C, 15°C) than at high temperature (25°C), consistent with a two-week delay in flowering time under field conditions in early spring when temperatures often fluctuate between near 2°C at night and above 25°C during the day.

To further determine whether the peach orthologs of the thermos-responsive regulatory genes exhibit altered expression

patterns in the LFP floral buds, a total of 84 transcriptomes were carefully analyzed and compared. These transcriptomes were derived from floral buds of both the JB and LFP accessions, which were subjected to various durations of chilling and warm treatments. Fig. 3a–e show that four of the six orthologs, including *ELF3*, *ELF4*, *LUX* and *PIF4*, were upregulated when the JB buds were transferred to the warm condition from the chilling condition. Four orthologous genes also showed similar responses in the LFP flower buds. Although *PhyB* barely responded to the chilling-to-warm transition (Fig. 3g), and *PhyA* was markedly downregulated (Fig. 6f), their expression response was invariant between the JB and LFP floral buds. Therefore, none of the peach orthologs showed apparent expression differences between genotypes (Fig. 6b–g). Further, we examined the sequences of six orthologous



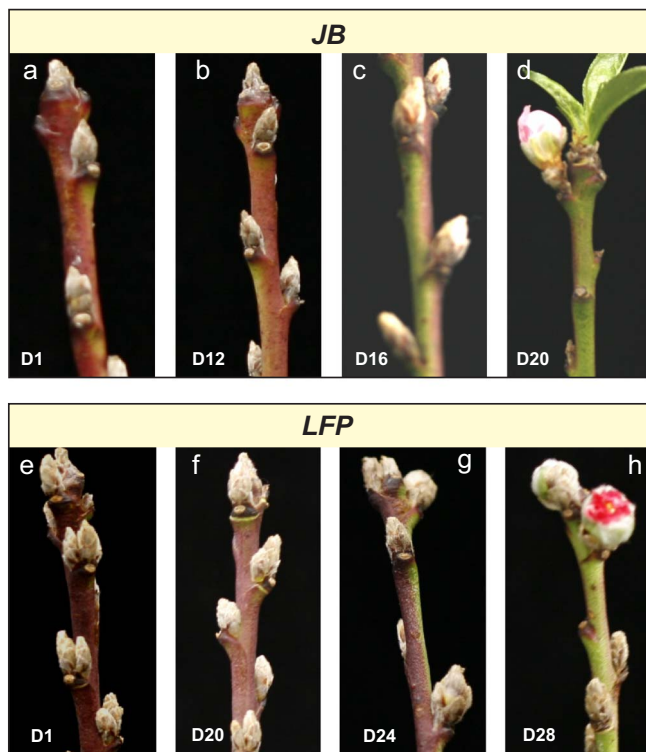


**Figure 2.** Flowering of the LFP buds required longer warm exposure. (a-h) The floral buds of JB (a-d) and LFP (c-h) peach were excised and fully chilled, before transferring to warm temperatures (~18–22°C). Floral bud break was evaluated at Day 1 (D1), Day 12 (D12), Day 16 (D16), Day 20 (D20), Day 24 (D24) and Day 28 (D28) for the JB (a-d) and LFP (e-h), respectively.

genes in *LFP* and *JB* genomes and found no sequence difference between the two genotypes for these genes (data not shown). Evidently, these six orthologous genes retain intact genomic sequences and expression profiles in the *LFP* flower buds.

### Potential candidate genes that control floral structures associated with late flowering trait

The *LFP* mutant displays an unusual increasing floral organ phenotype (Fig. 1m), which is similar to the altered floral organ phenotype observed in the *Arabidopsis pluripetala* (*plp*) and *enhanced response to abscisic acid1* (*era1*) mutants, both of which are defective in protein prenylation [38, 39]. This suggests that the *LFP* phenotype may be caused by a similar genetic defect as in the *plp* and *era1* mutants. The peach genome has orthologs of the corresponding genes, including one copy of *PLP/PRUPE\_1G191500* and two copies of *ERA1s*: *ERA1a/PRUPE\_3G284100* and *ERA1b/PRUPE\_6G347800*. Additionally, three prenylation-related genes, including *PRUPE\_2G233300*, *PRUPE\_2G11160*, and *PRUPE\_3G223100*, code for Rab-GGT  $\beta$  subunits of geranylgeranyltransferase and Rab geranylgeranyltransferase, respectively [39]. Recent studies showed that a dominant floral mutant with excessive petals, coined as double flower was triggered by a 994-bp deletion of the last exon of *PRUPE\_6G242400* coding for TOE-type AP2 factor designated *euAP2a* and the deleted region encompasses a miR172 target site [40]. The peach genome harbors two additional homologues, *euAP2b* (*PRUPE\_6G091100*) and *euAP2c* (*PRUPE\_6G231700*). Disruption of gene *PRUPE\_2G237700*, which encodes a miR172 variant, is also associated with a recessive double floral phenotype [41]. Thus, we anticipated that one of these genes could be a potential

candidate gene that regulates floral structure as well as late-flowering phenotype in *LFP* and they were analyzed in more details in the following analyses.

### Detection of the variation in expression associated with potential deletion and alternative splicing in candidate genes between *JB* and *LFP*

We next examined the differences in the expression of these candidate genes between *JB* and *LFP* floral buds. Of a total of 11 genes examined, including randomly selected *PRUPE\_2G206500* coding for a nuclear fusion defective 4 protein (NFD4), *ERA1b* was found to be the only gene that completely lost expression in the *LFP* floral buds under both chilling and warm conditions (Fig. 4c), followed by *Rab-GGT $\beta$ /PRUPE\_2G11160*, which was drastically downregulated in the same periods (Fig. 4e). Three genes, including *PLP/PRUPE\_1G191500*, *ERA1a/PRUPE\_3G284100* and *miR172/PRUPE\_2G237700* and *euAP2a/PRUPE\_6G242400* displayed preferential accumulation of RNA transcripts in the *LFP* buds during chilling treatment (Fig. 4a, b, h, i). The remaining genes showed little variation in expression between the *JB* and *LFP* floral buds during the treatment (Fig. 4a–k). To further investigate potential structural variations and alternative splicing patterns, we examined the RNA-seq data and found an absence of the accumulation of RNA reads across a large region internal to the 4-kb *ERA1b* region in *LFP* but not in *JB* buds (Fig. 4l, blue square), which is consistent with the observed loss of RNA expression (Fig. 4c). In addition, there was a read mapping variation in the last exon or exon 10 of *euAP2a* between *JB* and *LFP* floral buds (Fig. 4m, blue square), suggesting that a potential alternative splicing occurred in this region.

### Deletion of a 983-bp region within *euAP2a/PRUPE\_6G242400* was identified exclusively in the *LFP*, but not in the other 14 assembled peach genomes

To confirm sequence variation in the identified gene candidates, we sequenced and assembled the genomes of *JB* and *LFP* using Oxford Nanopore Technology, and identified the deletion of an internal 2456-bp segment within the 4-kb region of *ERA1b* and a 983-bp region within *euAP2* in the *LFP* genome (Fig. 4n). This 983-bp deletion was located in the same region as the 994-bp segment deleted in a peach double flower peach mutant [40]. The 983-bp deletion caused an alternative splicing of the 3' untranslated transcript, leading to a replacement of the last 80 amino acids in *euAP2a* with 24 different amino acids. However, the mutated *euAP2a* still contained the same first 387 amino acids that had all major domains such as two EARs, NLS, and AP2. The deletion also resulted in loss of the miR172 binding site in exon 10 and/or the miR172-mediated cleavage site in mutated *euAP2a* transcript, making the mutated *euAP2a* transcript resistant to miR172-mediated cleavage. Thus, this deletion leads to a gain-of-function mutation. Two A to C transversion point mutations were also identified in the *NFD4/PRUPE\_2G206500* coding regions of the *LFP* genome, which changed Arginine and Aspartic acid to Tyrosine and Lysine in *NFD4*, respectively (Fig. 4n). Further, a 10-bp insertion was found in the transcribed region of *PRUPE\_2G237700*, which codes for one of the five miR172 variants in peach [41, 42]. To investigate the potential correlation between a specific mutation event and the mutant flower/late-flowering phenotype in *LFP*, we examined sequence variations in an additional 13 publicly available assembled peach genome sequences (Fig. 4h), and found that the 983-bp deletion in *euAP2a/PRUPE\_6G242400* was present

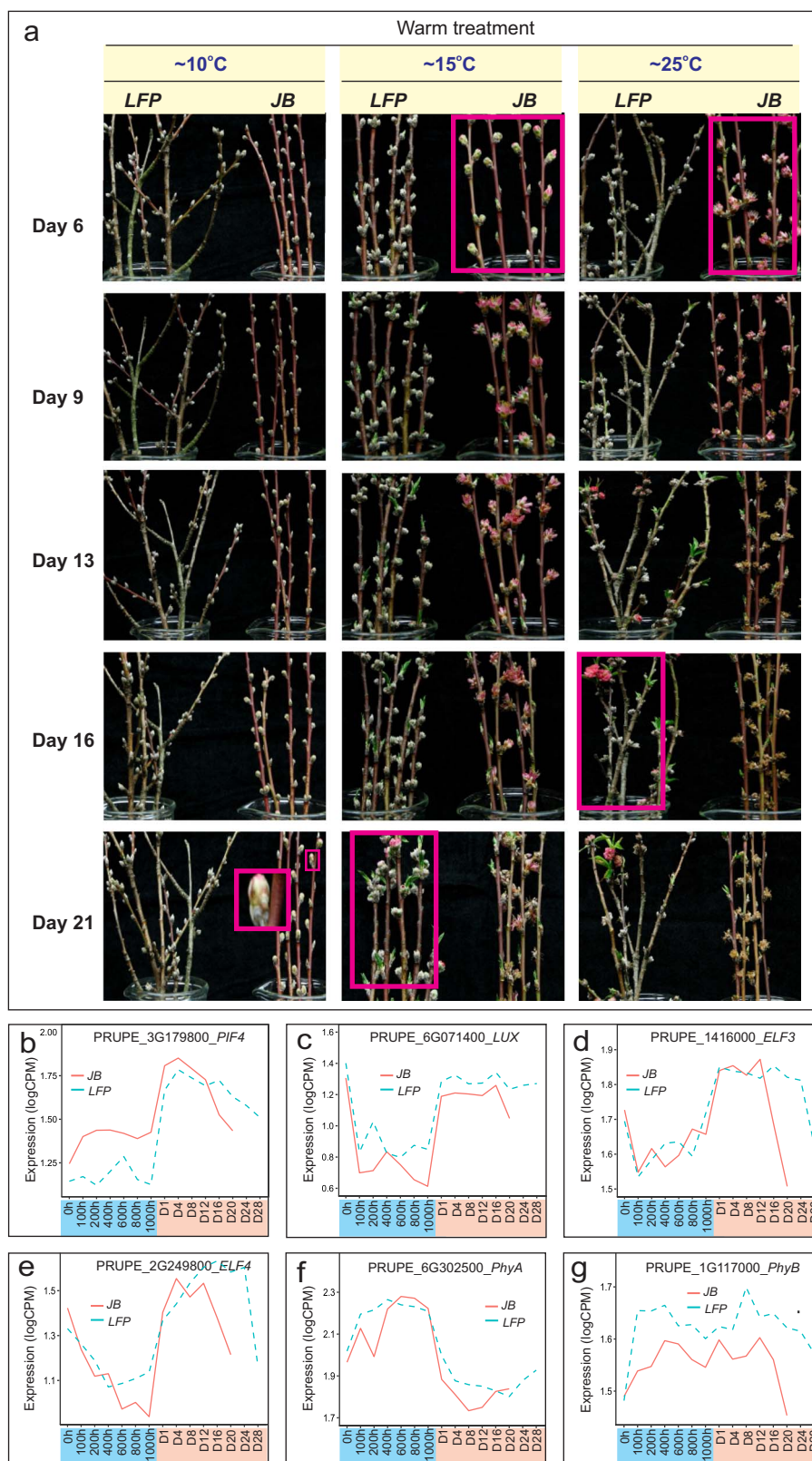


**Figure 3.** The slow response of LFP floral buds to various warm temperature regimes and the expression profiles of peach thermal-responsive flower regulator genes. **(a)** The fully chilled floral buds of JB (800 CH) and LFP (1,000 CH) were transferred to a growth chamber with temperatures set at 10°C, 15°C, and 20°C for 6, 9, 13, 16 and 21 days (Day 6, 9, 13, 16 and 21), respectively. **(b-g)** Expression profiles of genes PRUPE\_3G179800/PIF4 (b), PRUPE\_6G071400/LUX (c), PRUPE\_1G416000/ELF3 (d), PRUPE\_2G249800/ELF4 (e), PRUPE\_6G302500/PhyA (f) and PRUPE\_1G117000/PhyB (g).

only in the LFP, while other types of mutations such as the 2456-bp deletion within *ERA1b*, two point-mutations within *NFD4*, and the 10-bp insertion within PRUPE\_2G237700 were detected in at

least two of the 14 genomes (Fig. 4n). The 983-bp deletion was further examined in additional 46 unassembled peach genomes and none of them was found to carry the same deletion (Table S2).

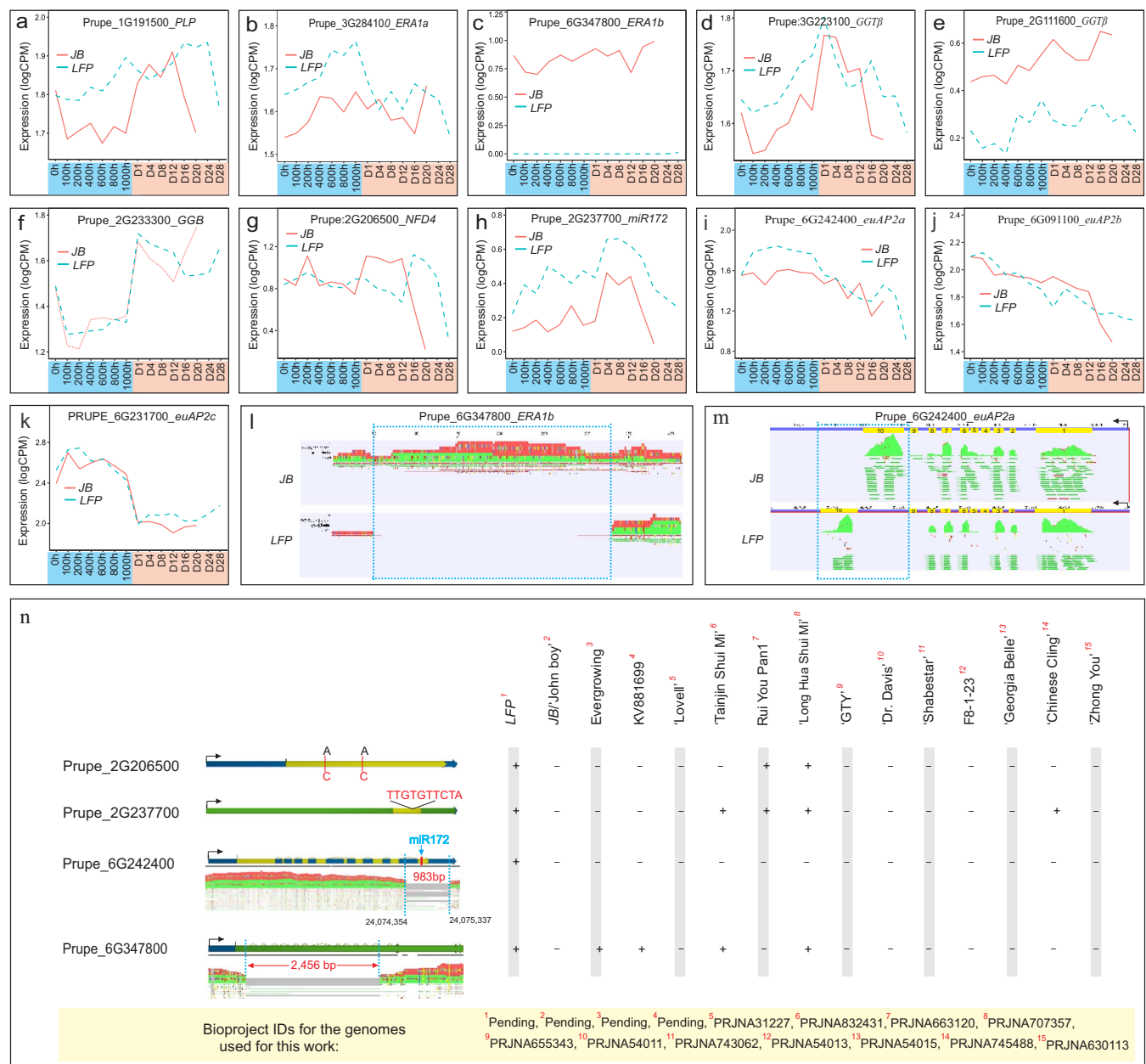


**Figure 4.** Association between the mutation of gene PRUPE\_2G242400/euAP2a, which as a 983-bp deletion and the mutant flower phenotype in the LFP. (a-k) Expression profiles of the indicated genes in floral buds during chilling (blue) and warm (light orange) treatments. (l-m) The alteration of RNA-seq read mapping pattern in PRUPE\_6G347800/ERA1b (l) and PRUPE\_6G242400/euAP2a (m) regions in LFP buds, respectively. The exon number and position on the euAP2a are indicated by number and highlighted in yellow. The absence of or altered read mapping pattern in the LFP flower buds are denoted by blue squares. Arrows indicate the gene transcription direction. (n) Survey of the genome sequence change in genes among 15 different assembled peach genomes. Two A to C transversions, one 10-bp insertion, and 983bp- and 2456bp-deletion events in four genes are depicted in the left panel, with (+) and (-) signifying the presence and absence of the mutation events in each genome. The Bioproject ID numbers (red) of each genome sequence are numbered and presented in the bottom panel.

This data, combined with earlier findings that the deletion of the 994-bp segment in the same region of PRUPE\_6G242400 instigates a double flower phenotype [40], supports that the 983-bp deletion is the main cause of the mutant flower morphology and the late-flowering trait in the LFP.

### Analysis of the transcriptomic landscape in LFP flower buds

A principal component analysis (PCA) revealed the overall transcriptomic relationships, with the first two components representing 70% and 10% of the total variations, respectively

(Fig. 5a). PC1 separated the 84 transcriptomes into chilling and warm clusters. JB and LFP genotypes formed distinct subclusters within the chilling cluster. According to PC2, the warm cluster can be further divided into two subgroups: early stage (Day 1 to Day 16/Day 24) and bloom day (Day 20/Day 28). There are two groups within the subgroup of bloom time between JB and LFP floral buds. Taken together, distinct transcriptomic relationships were delineated between different treatments and genotypes.

The global transcriptomic abundance in the LFP flower buds compared to that in the JB floral buds at 13 stages was analyzed, and 11541 differentially regulated genes representing 7837

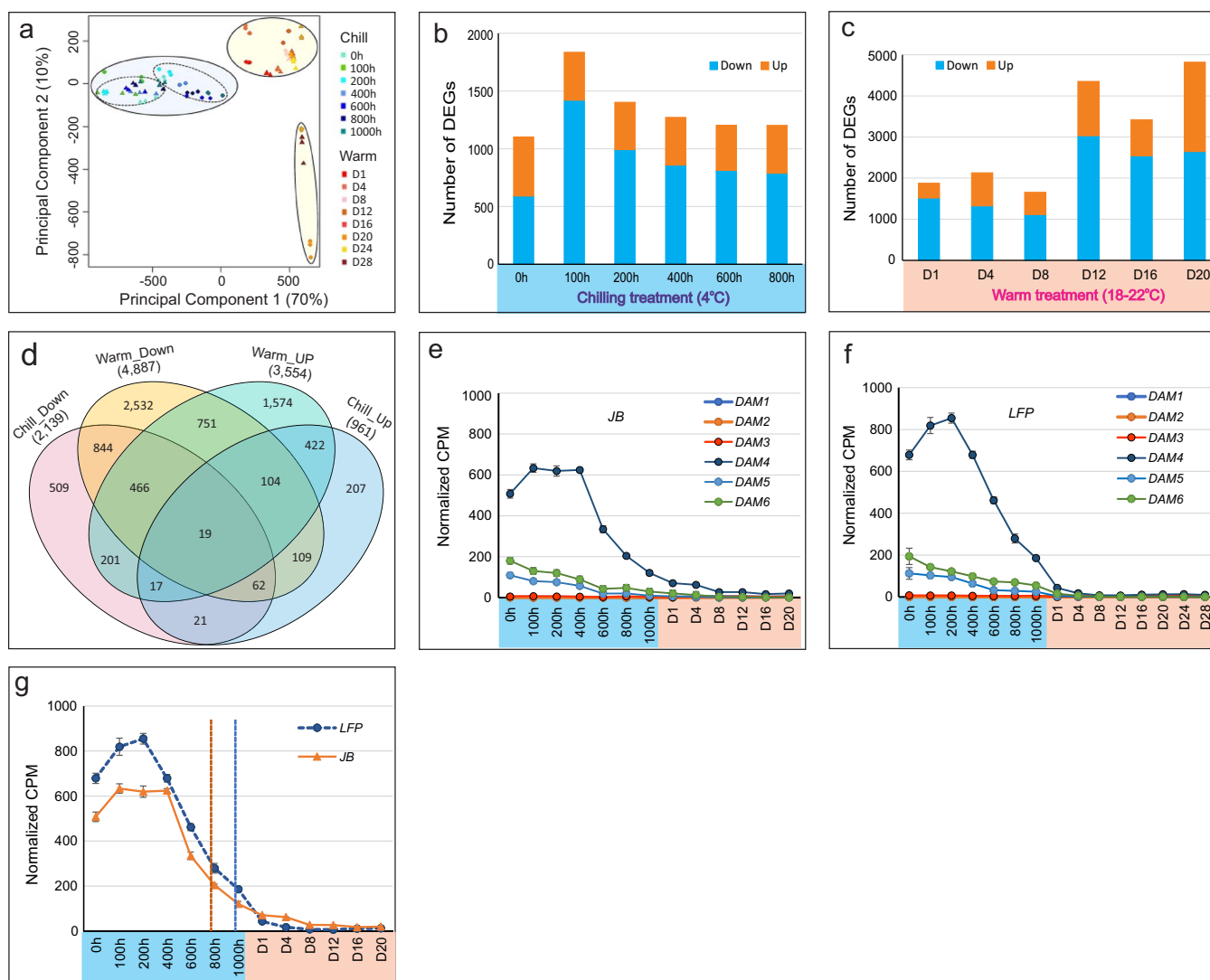


**Figure 5.** Changes in transcriptomic landscape between JB and LFP floral buds. (a) PCA showing the transcriptomic relationships. (b-c) Number of differentially expressed genes (DEG) (Down, down-regulated, and Up, up-regulated) in LFP compared to JB floral buds during chilling (b) and warm (c) treatments. (d-f) Altered expression amplitude and trajectory of DAM4 in JB and LFP flower buds.

unique ones were identified (Table S1), with 1103 to 1836 genes differentially regulated at each stage during chilling (Fig. 5b) and 1654 to 4821 genes differentially regulated during the warm period (Fig. 5c). A complex overlapping regulatory relationship led to multiple stages of intricate or opposite regulation for many of these genes (Fig. 5d). The expression of about 60% to 80% of genes in the LFP buds was lower than that of the JB floral buds, and only about 25% to 40% of them were higher during the chilling period (Fig. 5b). During the warm period, a similar expression trend was observed, especially from Day 1 to Day 16 (Fig. 5c), suggesting a fundamental transcriptomic change occurred in LFP buds. This transcriptomic change was also reflected in the regulation of some of the DORMANCY ASSOCIATED MADS-Box (DAM1–6) genes (Fig. 5e–g), which encode transcriptional repressors and regulate the chilling requirement for dormancy release and peach floral bud development [37]. In LFP buds, DAM4 upregulation occurred much faster, retained higher expression levels, and declined more slowly than in JB buds (Fig. 5e–g), which is coincident with its longer chilling requirement for exiting dormancy (Fig. 1).

### Stage-specific differential regulation of co-expression modules between the JB and LFP floral buds

To further explore the effect of *euAP2a* mutations on specific groups of genes, we classified 7837 DRGs into 19 co-expression modules using the TOMsimilarity algorithm in the weighted gene co-expression network analysis (WGCNA) [43], with the soft threshold selected to be 7 (Fig. S1). The size of the modules varied from 32 genes in M6 to 1808 genes in M16 (Fig. 6a; Table S3). By analyzing module–factor relationships, we correlated these modules with seven chilling stages and six warm stages. A module that correlates with a particular stage is red or dark red, indicating higher expression at that stage. Accordingly, at least eight modules in JB buds displayed high co-repression levels (Fig. 6a, left panel). In the heatmap, the red color intensity indicates that M9 was activated within the first 100 CH and continued to be upregulated until 200 CH before declining at 300 CH. Between 100 and 200 CH, M10 was also activated, suggesting M9 and M10 are chilling responsive. M2, M3, M4, M18 and M19 responded to warm temperatures exclusively, but at different



stages: M2 activated at Day 8 through Day 16, M19 at Day 12, M3 at Day 16, and M4 and M18 from Day 16 to 20, suggesting a transcription programming that is sequentially activated during flower development. These modules, however, dissipated or attenuated in the LFP floral buds at the same stages, which was particularly pronounced in M9, M10, M2, M3 and M4 (Fig. 6a, right panel). Figure 6b shows complete erasure of chilling-response in M9 and M10 modules but delayed activation of M2, M3, M4, M10 in LFP compared to JB flowers. The expression trajectory of the representative hub genes, which are those with high connectivity in each module (Fig. S2), further exemplified this differential regulation in Fig. 6c–g as activation of M2 was delayed from Day 4 in JB buds to approximately Day 16 in LFP buds, M3 from Day 8 to Day 20 and M4 from Day 12 to Day 24, respectively. A similar response was seen for M10 in JB buds on Day 1, but not in LFP buds until Day 12. Accordingly, mutation in *euAP2a* leads to a loss of chilling-responsive expression of M9 and M10, and a delay of warm-responsive expression of M2, M3 and M4 for 8 to 12 days, which coincides with the phenotypic delay of LFP bloom time (Fig. 2). It is noted that M10 is the only module that responded to both cold and warm temperatures at very early stages, which might play a key role in priming the initial thermal response in floral buds at early stages of the chilling and warm treatments.

GO network by Biological Networks Gene Ontology (BiNGO) [44] links genes to distinct biological processes, metabolic pathways, and floral developmental stages (Fig. 6h–l). The warm-responsive genes in the M2 module are associated with gametophyte and androecium development (Fig. 6h), while those in the M3 module are related to transport activity, fatty acid metabolism, floral morphogenesis, and pollen maturation (Fig. 6i). Additionally, the M4 group contains genes preferentially related to cell wall biosynthesis, cellular transport, and flower organ and gamete development, which are necessary for blooming, anthesis, and pollination (Fig. 6j). Furthermore, the chilling responsive M9 module mediates early stages of dormancy release and flower development, including cell wall biosynthesis, cellular transport, and floral structure development (Fig. 6k). PRUPE\_1G016700, the most abundantly expressed gene in the M9 group (Fig. 6f), encodes an acyl-CoA N-acyltransferase that plays a key role in maintaining developmental integrity of vegetative and inflorescence meristems in barley. The M10 module contributes to the modification of proteins and defense mechanisms (Fig. 6l), which are consistent with how it responds to low and high temperatures (Fig. 6l). All modules comprise distinct transcription factors that presumably activate and relay distinct regulatory cascades (Table S3). Floral development at the late stage is predominantly driven by M2, M3 and M4, while M9 likely initiates early transcriptional cascades and chilling-driven floral developmental programming [11–16].

### **A transient downregulation of *euAP2a* correlated inversely with stage-specific activation of five modules; however, this anti-relationship was absent from LFP floral buds**

The five co-expression modules underwent stage-specific, sequential activation throughout the entire chilling-warm treatment, suggesting that a coordinated transcriptional programming that drives floral developmental pace. The transient regulation of transcriptional cascades has been reported for some plant transcription factors, which transiently bind to DNA sequences [45, 46]. To understand whether the *euAP2a* is involved in this transient, stage-specific regulation, we examined *euAP2a* expression trajectory across 13 stages. During the chilling period,

the abundance of *euAP2a* transcript remained relatively constant in JB buds but was much greater in LFP buds (Fig. 4i). During the warm period, the difference disappeared as it promptly decreased in the LFP bud on Day 1 and continued declining in both JB and LFP buds onward (Fig. 4i). A similar pattern was observed in its two homologs, *euAP2b* and *euAP2c*, in JB and LFP buds, but their decline was much faster (Fig. 4j, k), suggesting that these three *euAP2s* share similar function. The detailed expression profile analysis revealed that the abundance of *euAP2a* transcript in JB buds declined moderately but transiently from 100 to 400 CH and reached its lowest level at 200 CH before rebounding to its normal levels at 400 CH. A similar expression dip was observed around Day 1, Day 8, and Day 16 in JB buds during the ensuing warm period, respectively (Fig. 7a, b, left bottom panels), which was barely present in *euAP2b* and *euAP2c* (Fig. 4j, k), suggesting that the stage-specific downregulation dynamic only occurred for *euAP2a*. Incidentally, these expression dips were associated with the activation of M9, M10, M4, M2 and M3 modules at specific stages in JB flower buds (Fig. 7b, c, left panels), indicating an anti-correlation expression between *euAP2a* and the five modules. However, in LFP flower buds, levels of *euAP2a* mRNA were increased, particularly during the chilling period, resulting in the disappearance of stage-specific dip patterns (Fig. 7b, right panel). Correspondently, the activation of M2, M3 was disrupted, and the activation of M4, M9, and M10 was delayed (Fig. 7b, c, right panels), suggesting that *euAP2a* acts as a transcriptional repressor in controlling chilling- and warm-responsive transcriptional programming during flower development.

## **Discussion**

Spring frost damage can be avoided by use of late-flowering traits in fruit trees, but these traits are scarce in the germplasm and the associated mechanisms are largely unknown. Using genetic, genomic, and molecular approaches, we have identified a mutation in *euAP2a* potentially associated with both flower morphology and delayed bloom date. We have also identified a unique regulatory relationship between *euAP2a* and five co-repression modules, as well as its relevance to the regulation of chilling requirements, floral development pace, and bloom times. These findings provide knowledge and insight for development of late flowering traits for improving fruit tree varieties to avoid spring frost damage.

Deletion of a 983-bp region at 3' *euAP2a* was both unique to LFP germplasm and displayed expression changes that tightly correlated with chilling/warming responses. The 983-bp deletion resulted in the loss of exon 10 where a miR172 binding site is located, and alternative splicing that creates a truncated protein with 24 different amino acids substituted for the last 80 amino acid residues in Wt *euAP2a*. An earlier study reported that a similar 994-bp deletion in the same region of *euAP2a* led to a dominant flower mutant with increased sepals, petals and stamens called double flower. It has been suggested that this is due to the loss of miR172-mediated translational repression or cleavage of *euAP2a* mRNA, assuming that the truncated *euAP2a* factor retains its full function [40]. In *Arabidopsis*, AP2 together with other factors specifies sepals and petal identity, and negatively interacts with AGAMOUS to control stamen and carpel formation [47]. However, AP2 is negatively regulated by miR172 that binds to the AP2 transcript and inhibits its translation (Chen, 2004). Mutation of miR172 binding sites often leads to an increase in AP2 translation/accumulation, resulting in a dominant proliferation of petals, stamens, and carpels [48, 49]. This is similar to the



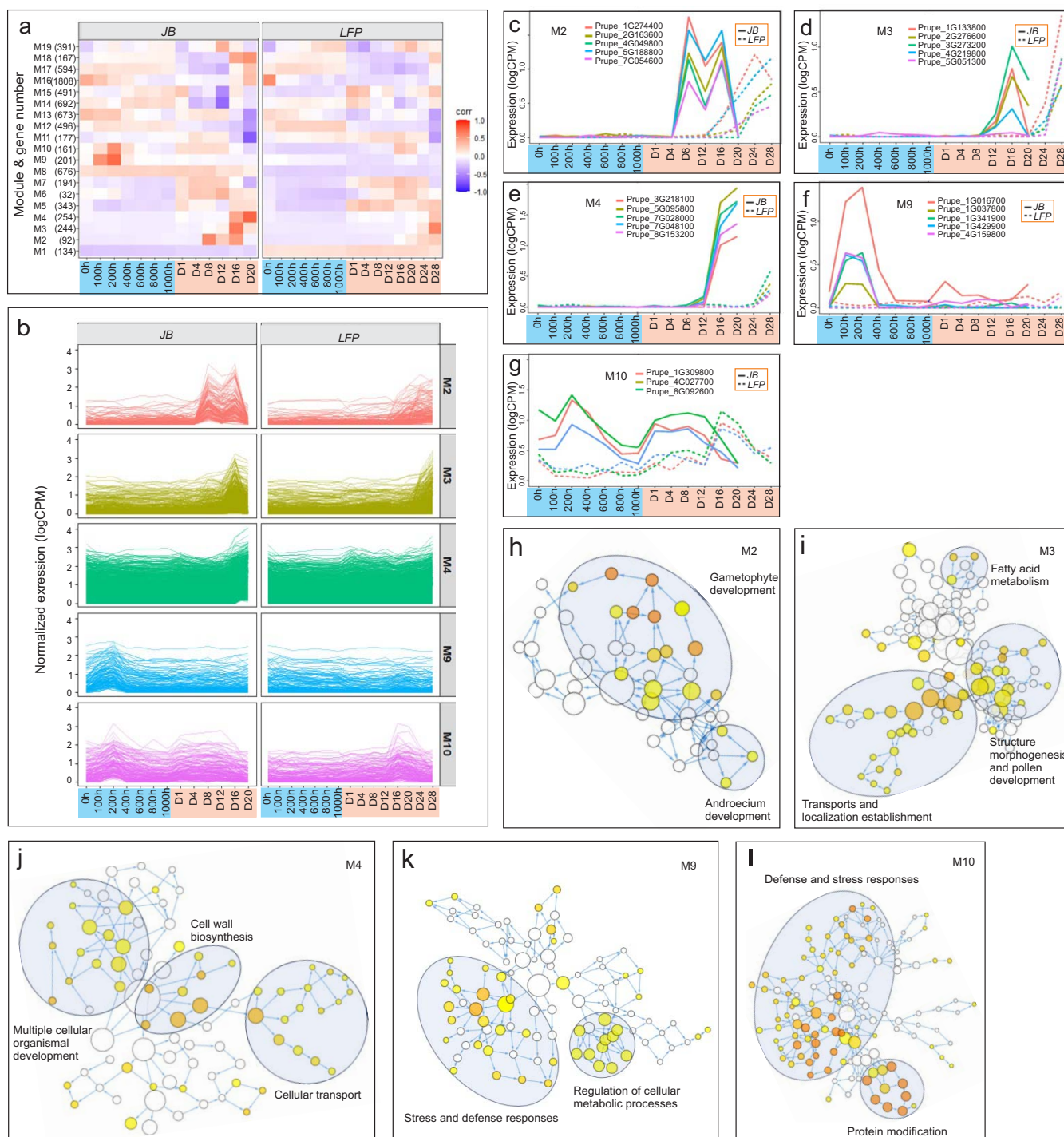


**Figure 6.** Differential regulation of co-expression modules in JB and LFP floral buds. **(a)** 19 co-expression modules, numbers of DEGs in each module and their differential regulation in JB and LFP floral buds. **(b)** Differential regulation of M2, M3, M4, M9 and M10 modules in JB (left panels) and LFP (right panels) floral buds, respectively. **(c-g)** Detailed analysis of expression trajectory of representative genes from M2 (c), M3 (d), M4 (e), M9 (f) and M10 (g) modules, respectively. **(h-l)** Enriched GO networks for five modules M2 (h), M3 (i), M4 (j), M9 (k) and M10 (l), respectively. Nodes represent individual GO terms, and node color indicates the p-value. General GO categories for nodes are labeled with ovals.

mutant phenotype observed in the double flower [40] and LFP peach plants, respectively. This evidence, together with our data, supports the notion that deletion of miR172 binding sites in exon 10 of *euAP2a* promotes floral organ proliferation (Fig. 1m; [23]).

In *Arabidopsis*, AP2 also represses flowering but this role is virtually masked by functional redundant AP2 domain-containing factors, such as TEMPRANILLO1 (TEM1) and TEM2 proteins [50], as

well as the TARGET OF EAT1 (TOE1) and TOE2, and the SCHLAFMUTZZE (SMZ) and SCHNARCHZAPFEN (SNZ), which belong to the euAP2 lineage [51–53, 55]. This repression role is manifested only in AP2-overexpressing plants that exhibit a late flowering phenotype or quadruple *smz snz toe1 toe2* mutants that display early flowering [51, 54–57]. In addition, the findings of [58] and [59] demonstrate a strong correlation between the number of

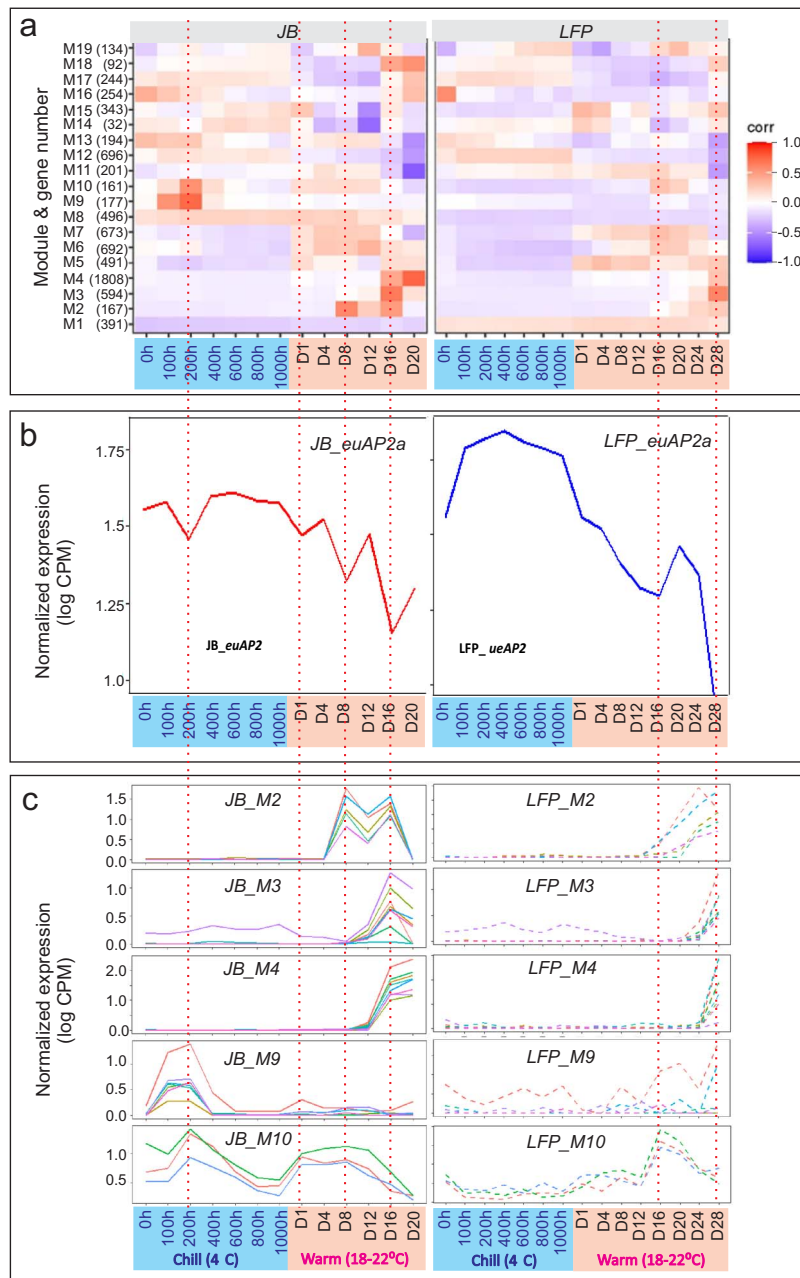


**Figure 7.** Mutation in *euAP2* erased its stage-specific transient downregulation trajectory and corresponding activation of five co-expression modules in LFP flower buds. **(a)** Association of the stage-specific dip in *euAP2* transcript abundance (bottom panels) with increasing heat map intensity/expression level of co-expression modules (top panels) in JB (left panel) or association of the loss of stage-specific down-regulation pattern of *euAP2* with lost or decreasing heat map intensity/expression level of co-expression modules in LFP (right panel) floral buds. **(b-c)** Plots of expression of representative genes from five responsive M2, M3, M4, M9 and M10 modules along 13 stages in JB (b) and LFP (c) floral buds, and their differential transcriptional activation response to changes in the *euAP2* stage-specific expression trajectory in LFP flowers.

floral petals and stamens in peach cultivars and their late flowering characteristics. These results, combined with the delayed flowering phenotype observed in *LFP* peach, provide supporting evidence that *euAP2a* functions both as a transcriptional activator, promoting floral organ proliferation, and as a repressor, inhibiting flowering time or development, thus acquiring canonical AP2's bifunctionality [49].

During dormancy release, winter chilling is known to drive cellular, tissue, and primitive morphological differentiation within peach floral buds [10, 11, 14, 18], which is crucial for synchronized and coordinated flower organ development under warm conditions. In light of the fact that the *LFP* floral buds

require much longer chilling periods (Fig. 1k), it is possible that the chilling-mediated regulatory mechanism may be compromised or altered as a result. In this study, we showed that chilling specifically activated the M9 and M10 modules immediately when dormant JB floral buds were exposed to cold conditions (Fig. 6a, f, g). The chilling-induced transient transcription in the *LFP* floral buds, however, was wiped out, indicating that mutation of *euAP2a* leads to impaired chilling-responsive transcription, resulting in a longer chilling period. The M9 module appears to be the only one involved in chilling-mediated biological regulation, as M10 transcription is sensitive to chilling and warm temperatures (Fig. 6f, g). In the M9 gene family, there are 201

genes that have been found to be enriched in cellular activity, stress and defense responses, and cell wall metabolism (Fig. 6k; Table S3). Accordingly, M9 genes play a role in resetting cellular hemostasis as well as active metabolic and physiological states. In barley, the ortholog of PRUPE\_1G016700 is crucial to the development of the inflorescence meristem, which is one of the most abundantly expressed genes in the M9 family, highlighting the role of the M9 module in floral meristem differentiation and development at early stages of chilling. It becomes apparent that *euAP2a* regulates chilling requirements and flower development at least via the modulation of the chilling-responsive M9 module activity.

When exposed to warm temperatures, only fully chilled floral buds become growth-responsive and resume bud development events such as successive bud enlargements, morphological changes, mature gametes, blooms, pollination, and fertilization. The delayed flowering time or longer warm period required for flower development and bloom in *LFP* trees suggests that the mutation in *euAP2a* delays or derails the warm-driven regulatory program, which is apparently supported by the transcriptomic analyses as evidenced by that upon exposure to warm temperatures, four co-expression modules of chilled *JB* floral buds were activated: M10 on Day 1 through Day 12, M2 on Day 4 through D16, M3 on Day 8 through D16, and M4 on Day 8 until bloom (Fig. 6b–e, g). Since these modules are sequentially activated at different stages of flower development, we believe they constitute major transcriptional programming to control flower developmental progress, but the mutations in *euAP2a* should interrupt the transcriptional programming pace, resulting in a later flowering phenotype. In line with the prediction, we found that the activation of all four modules under warm conditions was consistently delayed by at least eight days in *LFP* flowers versus *JB* buds (Fig. 6b–e, g), which is consistent with an 8-day delay in flowering (Fig. 2h). Hence, our work provided direct evidence that *euAP2a* targets or represses four modules at warm temperatures, highlighting the pivotal role of *euAP2a* in thermo-dependent transcription programming and floral development in deciduous fruit trees.

An inverse relationship was observed between the stage-specific activation of co-expression modules, and the transient downregulation of *euAP2a* (Fig. 7a–c, left panels), suggesting that *euAP2a* acts as a transcriptional repressor. This inverse correlation was further supported by the fact that the loss or delay of activation of the five modules was correlated with a loss or delay of the corresponding stage-specific downregulation trough of *euAP2a* transcripts in *LFP* floral buds (Fig. 7a–c, right panels). This again supports the negative regulatory function of *euAP2a*, which is consistent with previous findings in *Arabidopsis* that AP2 or AP2-related genes repress flowering ([51, 54–56]; Mathieu et al., 2009) as well as the transcription of the key flowering regulators SUPPRESSOR OF OVEREXPRESSION OF CONSTANS1(SOC1), AGAMOUS, and *miR172* genes [49].

Loss or delay of a transient, stage-specific downregulation of *euAP2a* transcript abundance in *LFP* buds and its rapid decrease under warm conditions suggest an intricate mechanism underlying *euAP2a* regulation. It is possible that a transient, stage-specific decrease in *euAP2* transcript abundance could be due to transient increase of *miR172* that may directly cleave *euAP2a* transcripts in *JB* peach floral buds, although an earlier study has shown that *miR172* primarily inhibits AP2 mRNA translation in *Arabidopsis* [56]. However, due to the deletion of *miR172* binding sites at the 3' of the *euAP2a* in *LFP* flower buds, its transcript would

become resistant to *miR172* cleavage, likely resulting in a greater abundance of *euAP2a* transcripts associated with attenuation or erasure of the stage-specific downregulation pattern in *LFP* buds under chilling conditions (Fig. 4i). However, under the warm condition, it changes and the *euAP2a* transcript abundance in *LFP* buds decreased rapidly within the first 24 hours after transfer to warm temperature, reaching a level similar to that in *JB* buds (Fig. 4i). Although the *euAP2a* transcripts decreased in both *JB* and *LFP* buds under warm conditions, the pattern and amplitudes varied, with *JB* buds still maintaining a transient dip-up regulation pattern until Day 16 while the *LFP* buds displaying continuous decrease, but slowly, until reaching a dip at Day 16 followed by another big dip from Day 24 to bloom day (Fig. 7a, b). Likewise, M10, M2, M3 and M4 activation was delayed or occurred on Day 16 and Day 24 in *LFP* buds instead of on Day 1, Day 4, and Day 16 in *JB* buds, respectively (Fig. 7b, c). This phenomenon raises the possibility that only *euAP2a* transcript abundance below a critical threshold could produce insufficient amount of *euAP2a* proteins for repression of these modules. In contrast, levels above the critical threshold could yield sufficient AP2 proteins to fully repress the modules' activation. This quantity-dependent regulation scenario appears to find experimental support in that AP2, which acts antagonistically and interacts with AGAMOUS to regulate floral organ identity in four floral whorls, can, when overproduced in *Arabidopsis*, supersede AGAMOUS function, causing homeotic conversion of AG-conferred stamens into AP2-specified petals, and other flower defects, respectively [47, 56]. Thus, *euAP2a* could, like the canonical *Arabidopsis* AP2, act in a quantity-dependent fashion to repress these co-expression modules.

The transient and stage-specific downregulation-mediated activation of five co-expression modules appears to be a unique feature of *euAP2a*, which has not been reported for AP2 or AP2-related transcription factors in other plants. This may be related to the 'hit-run' regulatory mechanism adopted by some plant transcription factors, which bind transiently to DNA sequences and activate transcriptional cascades, an action that cannot be captured by traditional transcriptomic analysis or stable ChIP-seq action [45, 46]. Nevertheless, we identified a strong candidate mutation that is responsible for both the double flower defect and the late-flowering trait in *LFP*, and also revealed a novel thermal-dependent transcriptional programming upon which *euAP2a* acts to control floral developmental progress under the chilling and warm conditions, respectively. Our findings will be instrumental in breeding or engineering the late flower traits in peach and other fruit crops.

## Materials and methods

### Peach mutants and chilling and warm treatments of the dormant floral buds Development of the late-flowering peach

The Late-flowering Peach (*LFP*; KV021779) was developed at the USDA-ARS Appalachian Fruit Research Station located at Kearneysville, WV. An initial cross was carried out between 'Flavortop' and Bologna Italian Pillar (pollen) to generate KV881475 which was then crossed with MA7-4-115 (pollen) to generate KV930605. A successive cross between KV930605 and WLFWNJ produced KV981637. The *LFP*/KV021779 line was selected from progenies of the open-pollinated KV981637 (Fig. 1a). Under Kearneysville's climate, *LFP*/KV021779 flowers at the end of April, which is about three to four weeks later than most peach cultivars, including 'John Boy', which was used as a control in this study.



### Determination of the chilling requirement

The LFP/ KV021779 and 'John Boy' trees are mature (fruit bearing) and have been subjected to standard management practices for pruning and pest/ disease management in the Mid-Atlantic region (e.g., 2023 Spray Bulletin for Commercial Tree Fruit Growers). The chilling requirement of the dormant peach floral buds was performed as described previously [37]. Briefly, shoots from LFP/ KV021779 and 'John Boy' with fully dormant floral buds were collected from the USDA-ARS-AFRS orchard (39.3578 N, -77.8845 W) at the end of October, and placed into a 20-L bucket with 2 to 4 cm of the cutting bases submerged in water at 4°C for various time periods up to 4 weeks before transferal to a room furnished with 16 h/8 h light/dark (fluorescent lighting, ca. 30 mmole photons  $m^{-2} sec^{-1}$ ) at 20 to 22°C. Water in the buckets was changed at least once every 4 to 5 days and ca. 1 cm of the shoot bases were cut off at the same interval to minimize bacterial growth and clogging of the xylem vessels. (Fig. 1). It was determined that 'John Boy' required 800 chilling hours, while LFP/KV021779 required 1000 chilling hours.

### Determination of the warm requirement

Per the chilling requirement data, 'John Boy' dormant floral buds were treated at 4°C for 800 chilling hours (CH) and LFP/KV021779 for 1000 CH to fully meet the chilling requirement, respectively, before being transferred to the warm condition for evaluation of bud break. The assay for the warm requirement was then carried out at 20 to 22°C and 16 h/8 h light/dark photoperiod (fluorescent lighting, ca. 30 mmole photons  $m^{-2} sec^{-1}$ ). Shoot maintenance, shoot cuts, and water change in buckets were performed per the chilling requirement.

The warm requirement determination was repeated with three different temperatures to assess the interaction of long day photoperiod and temperature as it relates to the warm requirement. The excised shoots with dormant floral buds were treated at 4°C for 800 CH ('John Boy') and 1000 CH (LFP) to fully meet the chilling requirement. The fully dormant shoots were then transferred to three growth chambers with temperatures set at ~10°C, ~15°C and ~25°C, respectively, with 60% humidity and 16 h/8 h photoperiod (fluorescent lighting, ca. 30 mmole photons  $m^{-2} sec^{-1}$ ). Shoot maintenance, shoot cuts, and water change in buckets were as described above. The bud development, break and blooming times were evaluated until day 21.

### Floral tissue collection, RNA isolation and RNA-seq analysis

During chilling treatment, floral buds of 'John Boy' and LFP were collected simultaneously at intervals of 200 CH (h) from 0 h until their CRs were met at 800 h and 1000 h, respectively. After transferring to warm conditions, florals buds were collected at 4-day (d) intervals until they started flowering on 20d and 28d, respectively. Samples were harvested from three trees as three independent biological replicates, thus making a total of 84 samples during the chilling and warm periods. Harvested samples were immediately frozen in liquid nitrogen, stored at -80°C until RNA extraction. RNA was isolated from ~50 mg of tissues using a Plant RNA Isolation Kit (Norgen Biotech Corp, Ontario, Canada) according to the provided protocol. RNA was eluted in 100  $\mu$ l of RNase-free inactivation reagent (Thermo Fisher Scientific, Waltham, MA, Cat# AM7006), and RNA quality and integrity was analyzed on a 1% agarose gel.

Between 500 and 800 ng of total RNA per sample was used to make RNA libraries using the Truseq Stranded mRNA Library Prep

Kit (Illumina) according to manufacturer instructions. Sequencing was performed on an Illumina NovaSeq S4 platform at Azenta Life Sciences (Burlington, MA, USA).

### Data and computation analyses

Raw reads from RNA-seq were filtered to remove low-quality reads and reads containing adaptor sequences or poly-N regions. Clean reads were aligned to the peach genome (Genome assembly *Prunus persica* NCBIv2, [https://0-www-ncbi-nlm-nih-gov.brum.beds.ac.uk/datasets/genome/GCF\\_000346465.2/](https://0-www-ncbi-nlm-nih-gov.brum.beds.ac.uk/datasets/genome/GCF_000346465.2/)) using STAR (v2.6.0; [60]). The mapped read counts were transformed to Counts per Million (CPM) using the Bioconductor package edgeR [61] for exploratory analysis and differential expression analysis. Differentially expressed genes (DEGs) were identified on genes with false discovery rate (FDR) < 0.05 and log fold-changes (logFC) > 1.5 between LFP and JB at each time point. The total identified DEGs from each time point of both chilling and warm treatment were analyzed using WGCNA [43] to detect co-expression modules. Network analysis and hub gene identification from selected modules were conducted using Cytoscape (v3.9, [62]). Gene Ontology (GO) analysis of the modules was performed using the Cytoscape plugin BiNGO [44].

### Genome sequencing of JB and LFP

Sequencing libraries were made with a Ligation Sequencing Kit (SQK-LSK110, Oxford Nanopore Technologies, Oxford, UK) and the sequencing was conducted on a miniON MK1B sequencer (MIN101-B, Oxford Nanopore Technologies) using a Nanopore R9.4.1 flow cell (FLO-MIN106D, Oxford Nanopore Technologies). The total number of reads and average read length were 2.0 Mb and 2216 bp for JB, and 3.4 Mb and 1708 bp for LFP. Based on a peach genome size of 220 Mb, the coverages were estimated to be 20.4X and 26.4X, respectively.

### Acknowledgements

This study was supported by USDA-ARS in-house funding under CRIS 8080-21000-029-00D and 8080-21000-033-00D.

### Author Contributions

Z.L. and C.D. conceived and designed experiments. J.L., D.D., M.D., T.A. E.B. and Z.L. conducted experiments. J.L., C.D., E.B. and Z.L. performed data analyses and data interpretation. Z.L., wrote the manuscript, and J.L., C.D., and T.A. assisted the manuscript preparation.

### Data availability

The raw and processed data from this study have been submitted to the NCBI BioProject and GEO databases, and accession number is GSE244570.

### Conflict of interest statement

The authors declare that they have no conflict of interest.

### Supplementary Data

Supplementary data is available at Horticulture Research online.

## References

- Liu J, Sherif SM. Combating spring frost with ethylene. *Front Plant Sci.* 2019;**10**:1408
- Bäurle I, Dean C. The timing of developmental transitions in plants. *Cell.* 2006;**125**:655–64
- Irish VF. The flowering of Arabidopsis flower development. *Plant J.* 2010;**61**:1014–28
- Sun L, Nie T, Chen Y. et al. From floral induction to blooming: the molecular mysteries of flowering in woody plants. *Int J Mol Sci.* 2022;**23**:10959
- Arora R, Rowland LJ, Tanino K. Induction and release of bud dormancy in woody perennials: a science comes of age. *HortScience.* 2003;**38**:911–21
- Atkinson CJ, Brennan RM, Jones HG. Declining chilling and its impact on temperate perennial crops. *Environ Exp Bot.* 2013;**91**:48–62
- Fan S, Bielenberg DG, Zhebentyayeva TN. et al. Mapping quantitative trait loci associated with chilling requirement, heat requirement and bloom date in peach (*Prunus persica*). *New Phytol.* 2010;**185**:917–30
- Erez A, Couvillon A, Hendershott CH. Quantitative chilling enhancement and negation in peach buds by high temperatures in a daily cycle. *J Am Soc Hortic Sci.* 1979;**104**:536–40
- Liu Z, Zhu H, Abbott A. Dormancy behaviors and underlying regulatory mechanisms: from perspective of pathways to epigenetic regulation. In: Anderson J, ed. *Advances in Plant Dormancy*. Springer Science, 2015,75–106
- Wang L, Zhang L, Ma C. et al. Impact of chilling accumulation and hydrogen cyanamide on floral organ development of sweet cherry in a warm region. *J Integr Agric.* 2016;**15**:2529–38
- Julian C, Rodrigo J, Herrero M. Stamen development and winter dormancy in apricot (*Prunus armeniaca*). *Ann Bot.* 2011;**108**:617–25
- Luna V, Lorenzo E, Reinoso H. et al. Dormancy in peach (*Prunus persica* L.) flower buds. I. Floral morphogenesis and endogenous gibberellins at the end of the dormancy period. *Plant Physiol.* 1990;**93**:20–5
- Luna V, Reinoso H, Lorenzo E. et al. Dormancy in peach (*Prunus persica* L.) flower buds. II. Comparative morphology and phenology in floral and vegetative buds, and the effect of chilling and gibberellin A3. *Trees.* 1991;**5**:244–6
- Luna V, Soriano MD, Bottini R. et al. Dormancy in peach (*Prunus persica* L.) flower buds. III. Levels of endogenous gibberellins, abscisic acid, indole-3-acetic acid, and naringenin during dormancy of peach flower buds. *Acta Hortic.* 1993;**329**:264–7
- Reinoso H, Luna V, Daurfa C. et al. Dormancy in peach (*Prunus persica*) flower buds. VI. Effects of gibberellins and an acylcyclohexanedione (trinexapac-ethyl) on bud morphogenesis in field experiments with orchard trees and on cuttings. *Can J Bot.* 2002a;**80**:664–74
- Reinoso H, Luna V, Pharis RP. et al. Dormancy in peach (*Prunus persica*) flower buds. V. Anatomy of bud development in relation to phenological stage. *Can J Bot.* 2002b;**80**:656–63
- Wang SP, Yuan CJ, Dai YT. et al. Development of flower organs in sweet cherry in Shanghai area. *Acta Hortic Sin.* 2004;**31**:357–9
- Yamane H, Tao R, Ooka T. et al. Comparative analyses of dormancy-associated MADS-box genes, PpDAM5 and PpDAM6, in low- and high-chill peaches (*Prunus persica* L.). *J Jpn Soc Hortic Sci.* 2011;**80**:276–83
- Ghrab M, Ben Mimoun M, Masmoudi MM. et al. Chilling trends in a warm production area and their impact on flowering and fruiting of peach trees. *Sci Hortic.* 2014;**178**:87–94
- Pawasut A, Fujishige N, Yamane K. et al. Relationships between chilling and heat requirement for flowering in ornamental peaches. *J Jpn Soc Hortic Sci.* 2004;**73**:519–23
- Ruiz D, Campoy JA, Egea J. Chilling and heat requirements of apricot cultivars for flowering. *Environ Exp Bot.* 2007;**61**:254–63
- Ruiz D, Egea J, Salazar JA. et al. Chilling and heat requirements of Japanese plum cultivars for flowering. *Sci Hortic.* 2018;**242**:164–9
- Alvarez-Buylla ER, Benítez M, Corvera-Poiré A. et al. Flower development. *Arabidopsis Book.* 2010;**8**:e0127
- Anderson JL, Richardson EA, Kesner CD. Validation of chill unit and flower bud phenology models for 'Montmorency' sour cherry. *Acta Hortic.* 1986;**184**:71–8
- Atagul O, Calle A, Demirel G. et al. Estimating heat requirement for flowering in peach germplasm. *Agronomy.* 2022;**12**:1002
- Luedeling E, Zhang M, Girvetz EH. Climatic changes lead to declining winter chill for fruit and nut trees in California during 1950–2099. *PLoS One.* 2009;**4**:e6166
- Alonso JM, Ansón JM, Espiau MT. et al. Stability of the almond blooming date in a changing climate. *Acta Hortic.* 2011;**912**:337–42
- Citadin I, Raseira MCB, Herter FG. et al. Heat requirement for blooming and leafing in peach. *HortScience.* 2001;**36**:305–7
- Scorza R, Okie WR. Peaches (*Prunus*). In: Moore JM, Ballington JR, eds. *Genetic Resources of Temperate Fruit and Nut Crops*. Vol. 290. 1st ed. Acta Horticulturae: Leuven, Belgium, 1991,177–234
- Jenkitkonchai J, Marriott P, Yang W. et al. Exploring PIF4's contribution to early flowering in plants under daily variable temperature and its tissue-specific flowering gene network. *Plant Direct.* 2021;**5**:e339
- Kumar SV, Lucyshyn D, Jaeger KE. et al. Transcription factor PIF4 controls the thermosensory activation of flowering. *Nature.* 2012;**484**:242–5
- Xu Y, Zhu Z. PIF4 and PIF4-Interacting proteins: at the nexus of plant light, temperature and hormone signal integrations. *Int J Mol Sci.* 2021;**22**:10304
- Box MS, Huang BE, Domijan M. et al. ELF3 controls thermoresponsive growth in Arabidopsis. *Curr Biol.* 2015;**25**:194–9
- Mizuno T, Nomoto Y, Oka H. et al. Ambient temperature signal feeds into the circadian clock transcriptional circuitry through the EC night-time repressor in Arabidopsis thaliana. *Plant Cell Physiol.* 2014;**55**:958–76
- Silva CS, Nayak A, Lai X. et al. Molecular mechanisms of evening complex activity in Arabidopsis. *Proc Natl Acad Sci USA.* 2020;**117**:6901–9
- Jung JH, Domijan M, Klose C. et al. Phytochromes function as thermosensors in Arabidopsis. *Science.* 2016;**354**:886–9
- Zhu H, Chen P-Y, Zhong S. et al. Thermal-responsive genetic and epigenetic regulation of DAM cluster controlling dormancy and chilling requirement in peach floral buds. *Hortic Res.* 2020;**7**:114
- Cutler S, Ghassemian M, Bonetta D. et al. SA protein farnesyl transferase involved in abscisic acid signal transduction in Arabidopsis. *Science.* 1996;**273**:1239–41
- Running MP, Lavy M, Sternberg H. et al. Enlarged meristems and delayed growth in plp mutants result from lack of CaaX prenyltransferases. *Proc Natl Acad Sci USA.* 2004;**101**:7815–20
- Gattolin S, Cirilli M, Pacheco I. et al. Deletion of the miR172 target site in a TOE-type gene is a strong candidate variant for dominant double-flower trait in Rosaceae. *Plant J.* 2018;**96**:358–71
- Cirilli M, Rossini L, Chiozzotto R. et al. Less is more: natural variation disrupting a miR172 gene at the di locus underlies the recessive double-flower trait in peach (*P. persica* L. Batsch). *BMC Plant Biol.* 2022;**22**:318

42. Zhu, H, Xia, R, Zhao, B. *et al.* (2012). Unique expression, processing regulation, and regulatory network of peach (*Prunus persica*) miRNAs. *BMC Plant Biol*, **12**.
43. Langfelder P, Horvath S. WGCNA: an R package for weighted correlation network analysis. *BMC Bioinformatics*. 2008;**9**:559
44. Maere S, Heymans K, Kuiper M. BiNGO: a Cytoscape plugin to assess overrepresentation of gene ontology categories in biological networks. *Bioinformatics*. 2005;**21**:3448–9
45. Alvarez JM, Schinke AL, Brooks MD. *et al.* Transient genome-wide interactions of the master transcription factor NLP7 initiate a rapid nitrogen-response cascade. *Nat Commun*. 2020;**11**:1157
46. Swift J, Coruzzi GM. A matter of time - how transient transcription factor interactions create dynamic gene regulatory networks. *Biochim Biophys Acta Gene Regul Mech*. 2017;**1860**:75–83
47. Wollmann H, Mica E, Todesco M. *et al.* On reconciling the interactions between APETALA2, miR172 and AGAMOUS with the ABC model of flower development. *Development*. 2010;**137**:3633–42
48. Mlotshwa S, Yang Z, Kim Y. *et al.* Floral patterning defects induced by Arabidopsis APETALA2 and microRNA172 expression in *Nicotiana benthamiana*. *Plant Mol Biol*. 2006;**61**:781–93
49. Yant L, Mathieu J, Dinh TT. *et al.* Orchestration of the floral transition and floral development in Arabidopsis by the bifunctional transcription factor APETALA2. *Plant Cell*. 2010;**22**:2156–70
50. Castillejo C, Pelaz S. The balance between CONSTANS and TEMPRANILLO activities determines FT expression to trigger flowering. *Curr Biol*. 2008;**18**:1338–43
51. Aukerman MJ, Sakai H. Regulation of flowering time and floral organ identity by a MicroRNA and its APETALA2-like target genes. *Plant Cell*. 2003;**15**:2730–41
52. Kim S, Soltis PS, Wall K. *et al.* Phylogeny and domain evolution in the APETALA2-like gene family. *Mol Biol Evol*. 2006;**23**:107–20
53. Park W, Li J, Song R. *et al.* CARPEL FACTORY, a dicer homolog, and HEN1, a novel protein, act in microRNA metabolism in Arabidopsis thaliana. *Curr Biol*. 2002;**12**:1484–95
54. Jung JH, Seo YH, Seo PJ. *et al.* The GIGANTEA-regulated microRNA172 mediates photoperiodic flowering independent of CONSTANS in Arabidopsis. *Plant Cell*. 2007;**19**:2736–48
55. Schmid M, Uhlenhaut NH, Godard F. *et al.* Dissection of floral induction pathways using global expression analysis. *Development*. 2003;**130**:6001–12
56. Chen, X. (2004). A MicroRNA as a Translational Repressor of APETALA2 in Arabidopsis Flower Development. *Science*, **303**, 2022–2025.
57. Mathieu, J, Yant LJ, Mürdter F. *et al.* (2009). Repression of Flowering by the miR172 target SMZ. *PLoS Biol*, **7**, e1000148.
58. Cirilli M, Micali S, Aranzana MJ. *et al.* The multisite PeachRefPop collection: a true cultural heritage and international scientific tool for fruit trees. *Plant Physiol*. 2020;**184**:632–46
59. Song YH, Niu L, Liu S. *et al.* Inheritance tendency of several characters of ornamental peach. *Acta Agric Sin*. 2010;**25**: 78–83
60. Dobin, A., Davis CA, Schlesinger F. *et al.* (2012). STAR: ultrafast universal RNA-seq aligner. *Bioinformatics*, **29**, 15–21.
61. Robinson, MD, McCarthy DJ, Smyth GK. *et al.* (2009). edgeR: a Bioconductor package for differential expression analysis of digital gene expression data. *Bioinformatics*, **26**, 139–40.
62. Shannon, P, Markiel A, Ozier O. *et al.* (2023). Cytoscape: a software environment for integrated models of biomolecular interaction networks. *Genome Res*, **13**, 2498–2504.
63. Wang Y, Georgi LL, Reighard GL. *et al.* Genetic mapping of the evergrowing gene in peach [*Prunus persica* (L.) Batsch]. *J Hered*. 2002;**93**:352–8